ingegneria sismica
International Journal of Earthquake Engineering
Anno XLIII - Num. 2 - 2026

Image Enhancement Based Fault Recognition Technology for Power Equipment in Low Illumination Environment

Yihui Zheng[1], *Chao Sun*[1,*], *Donghai Kuang*[1], *Yongbiao Liu*[1], *Peng Xu*[1] *and Hai Sun*[1]

[1] Guangdong Power Grid Co., Ltd. Guangzhou Power Supply Bureau, Guangzhou, Guangdong, 510000, China

SUMMARY: *This paper investigates intelligent enhancement techniques for low-light images based on deep learning. An image illuminance classification network was designed using an improved VGG network, with network width and depth pruning and the introduction of dilated convolutions to achieve lightweight network structure. By setting a probability threshold, low-light images are input into the subsequent image enhancement network for processing. Then, an image fault recognition method based on the VGG network + Retinex-Net and the improved YOLOv5 network is proposed. The analysis results show that the image fault recognition method proposed in this paper, based on Retinex-Net and the improved YOLOv5 network, can quickly and accurately detect and identify faults in power equipment.*

KEYWORDS: *image enhancement; YOLOv5 network; power equipment faults; recognition technology*

1 Introduction

In recent years, information technology and the economy have experienced rapid development, exerting a significant impact on various industries. However, this has also increased the load on power systems. The power grid is crucial to people's daily lives, industrial production, and the operations of government agencies, leading to heightened demands for the safety and reliability of power systems [1-3]. Within power systems, there are numerous critical components, such as transformers, transmission lines, and circuit breakers, which can influence and constrain the overall safe and stable operation of the power system [4]. Power equipment is a crucial component of the power system, and only when all types of equipment function normally can the grid maintain continuous output. However, these devices require prolonged operation and are mostly located outdoors, so the surrounding environment directly affects their stability, potentially causing various forms of damage or even failures [5-7]. Power equipment can experience a wide range of faults, and the factors contributing to these faults are also diverse. The primary causes include installation issues or power supply instability, external damage to transmission lines, and long-term operational factors such as insulation aging and overheating [8-11]. Statistics show that faults caused by power equipment issues account for approximately 70% of all cases. Mastering and analyzing power equipment is a very important part of improving fault identification capabilities to provide users with safe, high-quality, and economical power.

Traditional manual fault identification methods require specialized equipment for detection and demand a high level of professional expertise from staff, making it difficult to ensure

*tempmail0808@163.com
https://doi.org/10.65102/is2026660
Published: 30 April, 2026

identification efficiency. Additionally, in areas with complex terrain or low-light environments (such as at night, in tunnels, or in substation basements), these factors make manual fault identification complex and challenging [12]. With the continuous development of technology, scholars have developed various power equipment fault identification technologies that outperform manual fault identification. Zhao et al. [13] reported that compared to manual inspection, patrol robots improved the efficiency of substation equipment fault identification, and the support vector machine based on infrared images achieved an accuracy rate of up to 97% in fault identification. Sun et al. [14] used tunnel robots equipped with audio signal processing and intelligent monitoring to inspect indoor substation equipment, achieving low-cost and convenient fault identification for substation equipment. Yao and Wu [15] developed a fault identification technology for power transformers, combining infrared power image data with fault temperature thresholds and temperature change rates as data references to identify faults. Meradi et al. [16] used an electrical measuring instrument to measure the voltage of medium-voltage underground power cables and classified the measurement data using machine learning to achieve accurate identification and localization of cable faults. Wu et al. [17] applied deep learning technology to detect and diagnose power equipment faults, effectively improving fault identification accuracy and efficiency while reducing equipment maintenance costs. Liu et al. [18] utilized YOLOv4 (You Only Look Once 4) to construct an infrared image-based object detection model for locating and identifying fault hotspots in power equipment, achieving an accuracy rate of 92.2%. Li et al. [19] employed a backpropagation neural network to identify wear-related gear faults and rolling bearing faults in wind turbines within wind power generation equipment, achieving identification accuracy rates exceeding 95% in both cases. Liu et al. [20] designed a lightweight residual dense convolutional neural network model integrating transfer learning strategies and attention mechanisms using energy spectra and deep learning for identifying power equipment faults, achieving an identification accuracy rate of 99.4%.

Additionally, Liu et al. [21] processed the contours of thermal imaging and visible light images to construct an instance segmentation network. Training on datasets under different time and weather conditions demonstrated that this segmentation network can be used to identify abnormal heating in high-voltage power equipment. Zhou et al. [22] combined superpixel segmentation technology and residual networks to process infrared images of transmission lines, enabling effective automatic identification, classification, and localization of transmission line faults. Guan et al. [23] proposed a deep convolutional neural network-based early fault identification technology for substation equipment, utilizing transfer learning to extract equipment image features, and combining convolutional neural networks with two fully connected neural network layers for efficient and accurate fault classification, thereby achieving fault identification. Zhong et al. [24] introduced the Transformer model, transfer learning, and generative adversarial networks to enhance the recognition performance of drone images, thereby improving the accuracy and efficiency of smart grid equipment fault detection. Zhao et al. [25] enhanced the quality of nighttime power line images using an adaptive transformer-image processor module, convolutional neural networks, and the Transformer model. Combined with an improved YOLOv7, this approach enables efficient and accurate identification of nighttime power line insulators. It is evident that image quality enhancement processing of power equipment images is an effective method for improving equipment fault identification performance.

With the rapid development of intelligent technology, image enhancement techniques have taken on an important role in the field of image processing. Images obtained through various means can be processed through appropriate enhancement techniques to transform originally

blurry or even indistinguishable raw images into clear, information-rich usable images. This effectively removes noise from images, enhances edges or other regions of interest, and facilitates the detection and measurement of target objects within images. Such techniques have penetrated fields such as medical diagnosis, aerospace, military reconnaissance, fingerprint recognition, non-destructive testing, and satellite image processing [26-30]. Liu et al. [31] used partial differential equations to enhance the texture details and brightness of infrared images and improved infrared image segmentation methods, achieving significant quality enhancement effects on infrared images of power equipment. Yuan et al. [32] designed a low-light image enhancement method that utilizes contrast-limited adaptive histogram equalization to enhance the brightness and contrast of drone images while suppressing noise, effectively improving object detection in images of overhead power transmission systems, with insulator detection accuracy improved by 24%.

First, the paper constructs a low-light image classification network based on an improved VGG network to distinguish between low-light and normal-light images. Then, by constructing Retinex-Net and Zero-DCE networks, the paper designs a network loss function. The effectiveness of the method is verified through experimental testing on public datasets and in actual power equipment application environments. Furthermore, to improve the accuracy and speed of fault detection in power equipment images, a method based on the VGG network + Retinex-Net and an improved YOLOv5 network is proposed for image fault detection. The improved VGG network with a normalization layer is used to distinguish low-light images from normal-light images in inspection images. The Retinex-Net network is employed to enhance low-light images. The YOLOv5 network is improved through loss function optimization, convolution enhancements, and the introduction of a convolutional attention mechanism module. The enhanced low-light images and normal images are then subjected to fault identification. Finally, performance testing experiments are conducted on the improved power fault identification algorithm.

2 Research on low-light image enhancement methods based on deep learning

By leveraging artificial intelligence technology and applying deep learning to low-light image enhancement, the quality of enhanced low-light inspection images can be improved, thereby providing better technical support for power line fault detection. This paper first employs an improved VGG image illuminance classification network to screen low-light images. Then, we construct the strongly supervised network Retinex-Net and the weakly supervised network DCE-Net, set hyperparameters based on the original network structure, determine the loss function, and finally complete network training to achieve intelligent low-light image enhancement based on different algorithm theories. By establishing an evaluation system for enhancement effects, we compare the image enhancement performance of the two networks to determine the final enhancement network, thereby achieving end-to-end image enhancement operations.

2.1 Research on Image Illuminance Classification Methods Based on Improved VGG Networks

2.1.1 Network Structure Design

To quickly and intelligently distinguish between low-light and normal-light images, this paper designs an image illuminance classification network. Images obtained through inspections are

first processed by the image illuminance classification network for classification. Images classified as low-light are input into the subsequent low-light image enhancement network for image enhancement. Images classified as normal illumination are directly fed into the fault detection network for training. Since this task essentially falls under a binary classification problem, the network structure does not need to be overly complex. This paper proposes an improved VGG classification network. The network structure diagram is shown in Figure 1.

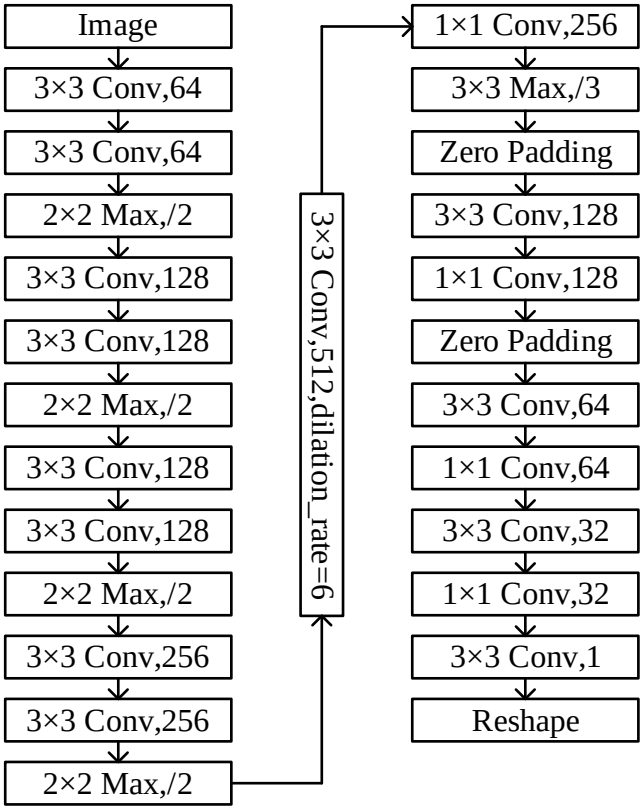

Figure 1: Improved VGG Network Structure diagram

2.1.2 Network Training

The image inputs for the low-light image classification network are sourced from the LOL dataset and the Brightening Train dataset. The LOL dataset, also known as the “Low Light Pairing” dataset, contains 500 normal/low-light image pairs obtained from real-world scenes for strongly supervised training [33]. By fixing the camera position and varying only the exposure time and ISO sensitivity, a large number of low-light images were captured of the same scene. The dataset includes images captured from various scenes such as pools, desks, kitchens, and streets.

The Brightening Train dataset first collects 270 low-light images from public datasets such as MEF, NPE, LIME, DICM, VV, and Fusion, converts the images to YCbCr channels, and calculates the Y channel. Then, 1,000 original images are collected from RAISE as normal-light images, and the histogram of the Y channel in YCbCr is calculated. By adjusting various parameters in the synthesized low-light images to make their Y channel histograms match the results in the low-light images, the illuminance distribution of the synthesized images is made to match that of the low-light images. Finally, the sizes of these original images are adjusted to the network input size and converted into the graphical format for input to the network.

The loss function for the low-light image classification network is the binary cross-entropy loss function:

$$L = -\frac{1}{m}\sum_{i=1}^{m}[y_i \log h_w(x_i) + (1-y_i)\log(1-h_w(x_i))] \tag{1}$$

In the formula:

y_i ——true label of the image.

x_i ——input image.

2.2 Low-light image enhancement processing based on Retinex-Net

2.2.1 Network Structure Analysis and Construction

This paper first analyzes and constructs the Retinex-Net low-light image enhancement network [34]. This network integrates image decomposition and subsequent enhancement operations. The Retinex-Net network introduces the traditional human color perception Retinex theory into deep learning. This theory assumes that the observed image can be decomposed into two parts: the reflected image and the illuminated image. Let s represent the source image, which can be expressed as:

$$S(x, y) = R(x, y) * I(x, y) \tag{2}$$

In the equation:

R — reflected image.

I — illuminated image.

The reflected image describes the intrinsic properties of the captured object, which are considered consistent under any brightness conditions. The illuminated image represents the light source describing the object's surface and the brightness information of the environment when the image is captured. In low-light images, dark and unbalanced lighting distributions are commonly encountered. Inspired by Retinex theory, Retinex-Net performs reflection/ illumination decomposition tasks in the decomposition network and achieves low-light enhancement in the enhancement network.

In the decomposition network, Decom-Net decomposes the training images into reflection images and illumination images. In the adjustment step, the Relight-Net network, based on an Encoder-Decoder structure, enhances the illumination images. Finally, the adjusted illumination images and reflection images are reconstructed to obtain the enhanced results. The network structure diagram is shown in Figure 2. Under the constraint that low/normal illumination images share the same reflectance image and illumination image smoothness, Decom-Net extracts the same reflectance image from different illumination images through network training.

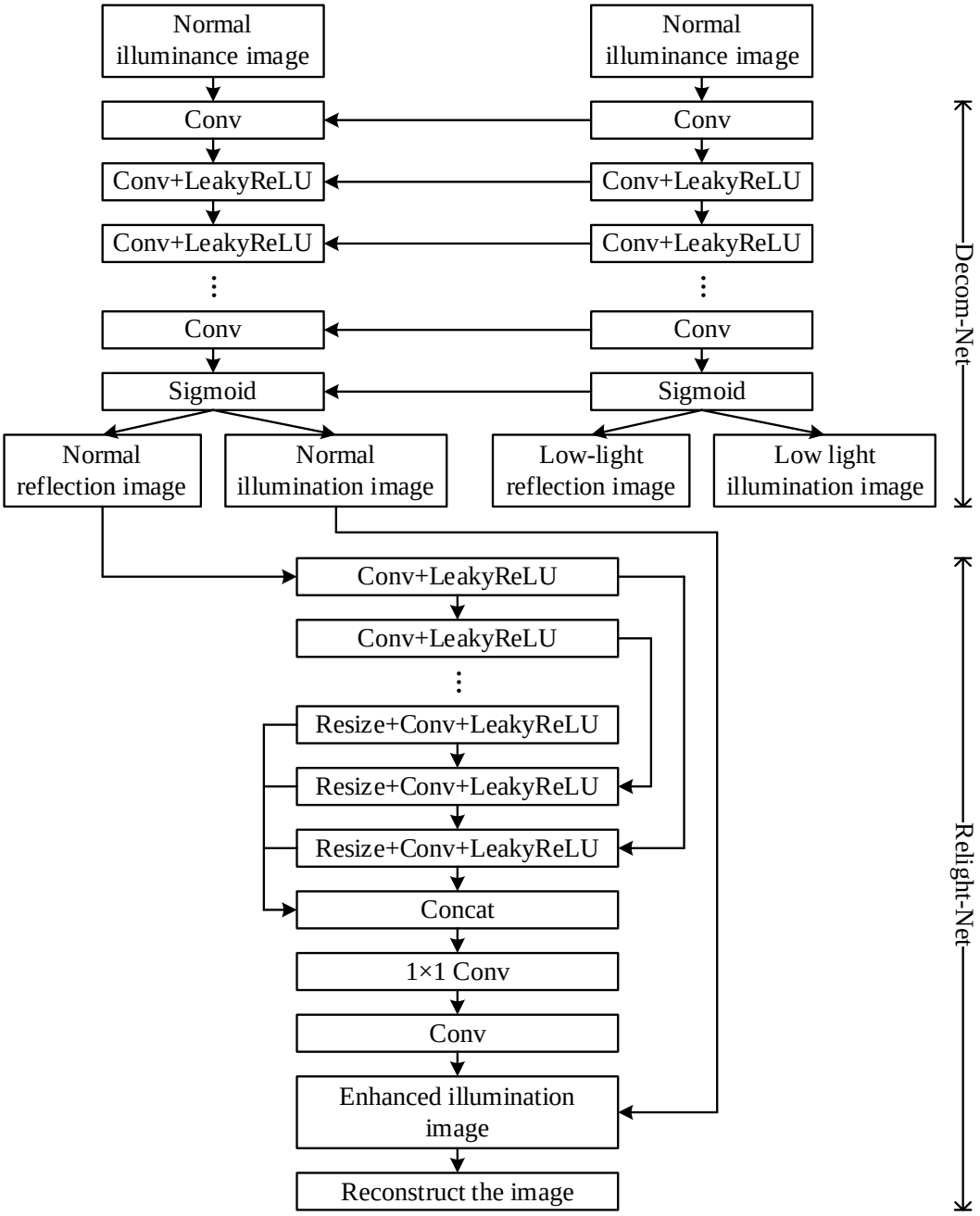

Figure 2: Schematic Diagram of the Retinex-Net network structure

The Relight-Net module enhances low-illumination images obtained through decomposition using an Encoder-Decoder structure. This structure introduces skip connections to establish channels between feature maps of the same scale, enabling feature superposition at the pixel level. This approach addresses the issue of gradient vanishing caused by convolutional layer superposition while facilitating gradient backpropagation, thereby accelerating network convergence. Relight-Net takes low-illumination images Ilow as input, first passing through downsampling layers to obtain illumination information from large-scale feature maps, then reconstructing local illumination information through upsampling operations. Each convolutional layer is configured with 64 3×3 convolutional kernels. Finally, a 1×1 convolutional kernel is applied to compress the number of channels, simplify features, and obtain the final reconstructed illumination image.

2.2.2 Determination of loss function

The loss function of the decomposition network consists of three parts: the reflection image consistency loss function, the lighting image smoothness loss function, and the reconstruction loss function. The calculation formulas are as follows:

$$L = L_{recon} + \lambda_{ir} L_{ir} + \lambda_{is} L_{is} \tag{3}$$

In the equation,

L_{recon} — reconstruction loss function.

L_{ir} — reflected image consistency loss function.

L_{is} — Illumination image smoothness loss function.

$\lambda_{ir}, \lambda_{is}$ — Loss ratio balancing factors.

The reconstruction loss function is as follows:

$$L_{recon} = \sum_{i=low,normal} \sum_{j=low,normal} \lambda_{ij} \| R_i \cdot I_j - S_j \|_1 \tag{4}$$

In the equation, λ_{ij} is the modulation coefficient, and $\lambda_{ij} = 0.001$.

From the above equation, it can be seen that both the low-illumination reflection image R_{low} and the normal-illumination reflection image R_{normal} can be multiplied by the corresponding illumination image to reconstruct the original image.

The reflectance consistency loss function is as follows:

$$L_{ir} = \| R_{low} - R_{normal} \|_1 \tag{5}$$

The lighting image smoothness loss function is implemented based on the gradient weighting of the reflection image in the horizontal and vertical directions. Under the influence of the exponential term, the areas with large gradients in the reflection image are constrained. The loss function can be expressed as:

$$L_{is} = \sum_{i=low,normal} \| \nabla I_i \cdot e^{-\lambda_g \nabla R_i} \|_1 \tag{6}$$

In the equation,

∇ — gradient in the horizontal and vertical directions.

λ_g — structure-aware intensity balance coefficient, $\lambda_g = 10$.

The loss function L of the illumination image enhancement network consists of the reconstruction loss L^I_{recon} and the illumination image local smoothing loss function L_{is}. L^I_{recon} represents the generation of a normal illumination image, i.e.:

$$L^I_{recon} = \| R_{low} \cdot \hat{I} - S_{normal} \|_1 \tag{7}$$

In the formula, $\hat{I}$ is the gradient weight of R_{low}.

3 Experimental results and analysis

To validate the effectiveness of the proposed algorithm, this section compares it with traditional image enhancement algorithms from recent years on both public datasets (SUNRGB-D dataset) and real-world power equipment data. The compared algorithms include NPE, LIME, HE, MSRCR, WV_SIRE, and ALSM. The images selected from the SUNRGB-D dataset are all from everyday life scenes, and each image has the characteristics of low illumination and uneven lighting. The power equipment data collection images are all collected from actual application scenarios.

3.1 Experimental Environment

All experiments in this section were conducted on a Windows 10 system with the following hardware configuration: NVIDIA GeForce GTX 1650 Ti GPU with 8 GB of memory; AMD Ryzen 7 4800H CPU with 16 GB of memory. To ensure consistency in the experimental environment for the algorithms described in this paper and the comparison algorithms, all experiments in this section were programmed using Matlab 2018b software.

Additionally, the algorithm proposed in this paper primarily includes three parameters: Gaussian standard deviation σ, reflection component transmission adjustment factor ω, and kernel window ω. To obtain more accurate illumination components, the parameter σ must be set. In the algorithm presented in this paper, the parameters σ_1 and σ_2 are set to 141 and 239, respectively. Additionally, to better constrain the local similarity of the reflection components, the adjustment factor ω is set to 0.5, while the kernel window size Ω is uniformly set to 7×7.

3.2 Quantitative comparative assessment

This section evaluates the enhanced results of the proposed algorithm using the Blind Image Anisotropic Quality Assessor (BIQAA), Fuzzy Cumulative Probability Density (CPBD), Reference-Free Spatial Domain Image Quality Assessor, and Natural Image Quality Evaluator (NIQE) as objective evaluation metrics.

Quantitative comparison experiments were conducted on the SUNRGB-D dataset and real-world power equipment data. The comparison of objective quality evaluation metrics on the SUNRGB-D dataset is shown in Table 1. The comparison of objective quality evaluation metrics in the power equipment environment is shown in Table 2. The Biased Image Quality Assessment (BIQAA) performs unbiased image quality assessment by measuring the variance of the expected entropy of a given image across a set of predefined directions. It uses the spatial frequency distribution as an approximation of the probability density function for local calculations to obtain the image entropy value. For enhanced images, the higher the BIQAA value, the better the details are preserved in the enhanced image, and the more prominent the local texture information becomes. As shown in Table 1, similar to the qualitative comparison analysis, ALSM has the highest entropy difference value, enabling better highlighting of image texture details after enhancement. In contrast, although the proposed algorithm in this paper has a suboptimal value, it achieves the optimal metrics in CPBD, BRISQUE, and NIQE, enabling the enhanced image to better balance image detail enhancement and naturalness retention.

Table 1: Comparison of objective quality evaluation metrics in the SUNRGB-D dataset

Methods	NPE	LIME	HE	ALSM	MSRCR	WV_SIRE	Proposed
BIQAA	0.0077	0.0105	0.0108	0.0154	0.0021	0.0104	0.0137
CPBD	0.5697	0.5631	0.5684	0.5551	0.5597	0.5577	0.5869
BRISQUE	37.3091	37.5752	36.7761	34.5357	33.7843	33.175	29.0095
NIQE	3.4222	3.2728	3.3504	3.6378	3.8211	3.6624	2.9912

A reference-free target sharpness measurement index (CPBD) based on the cumulative probability of blur detection is proposed. This index evaluates image sharpness by considering the human visual system's (HSV) response to blur distortion. For different enhancement results, the larger the CPBD index, the better the image's edge structure information is retained. As shown in Table 1, compared to other algorithms, the CPBD metric of the proposed algorithm achieves the highest value, indicating that the proposed algorithm can better sharpen image edges after enhancement, resulting in clearer enhancement results and higher image quality. The BRISQUE (Binary Regional Image Quality Estimator) metric utilizes the property that distortion alters the brightness normalization coefficient of an image to assess visual image quality. For experimental results, a lower BRISQUE value typically indicates a lower brightness distortion rate in the enhanced image. As clearly shown in the experimental results of Tables 1 and 2, the enhanced results of the algorithm proposed in this paper have the lowest BRISQUE values, indicating that after enhancement by the algorithm proposed in this paper, the brightness distortion rate is lower, and the enhanced results can better preserve the natural brightness of the image.

Table 2: Comparison of objective quality evaluation indicators

Methods	NPE	LIME	HE	ALSM	MSRCR	WV_SIRE	Proposed
BIQAA	0.0064	0.0074	0.0083	0.0068	0.0022	0.0084	0.0089
CPBD	0.5222	0.5184	0.5085	0.4891	0.5221	0.4427	0.5155
BRISQUE	34.8696	33.2804	30.7753	34.5704	31.3931	32.1838	29.4529
NIQE	3.2468	3.2514	3.2331	3.5783	3.8135	3.879	3.1763

The Natural Image Quality Evaluator (NIQE) extracts perceptual quality features of an image using a natural scene statistical model, fits a multivariate Gaussian model based on these features, and finally measures image quality by calculating the distance between the parameters of the distorted image and the natural image. A smaller NIQE value indicates that the enhanced image appears more natural to the human eye. As shown in the experimental results presented in Table 2, the algorithm proposed in this paper achieves the lowest NIQE value, effectively preserving the naturalness of the image after enhancement, with improved color saturation and better visual perception.

A comprehensive comparison of the above four objective evaluation metrics reveals that, compared to current image enhancement algorithms, the proposed algorithm not only effectively suppresses noise while enhancing image texture details and improving brightness and contrast, but also preserves the naturalness of the enhanced image, achieving excellent performance in both qualitative and quantitative evaluations.

Additionally, execution efficiency is another important metric for evaluating the performance of low-light image enhancement algorithms. To further validate the real-time performance of the proposed algorithm in practical application scenarios, a performance comparison was conducted on existing algorithms processing images of different sizes. The average execution times of different algorithms are shown in Figure 3. As the image resolution

increases, the HE algorithm has the shortest average execution time, consistently under 1 second; however, its enhancement effects are often suboptimal, with the enhanced images prone to color shifts. The method proposed in this paper is similar to the WV_SIRE algorithm in terms of execution efficiency, but as shown by the objective quality assessment metrics listed in Tables 1 and 2, the proposed method achieves the best enhancement results. Therefore, considering both execution time and enhancement effectiveness, the proposed algorithm strikes an acceptable balance between the two.

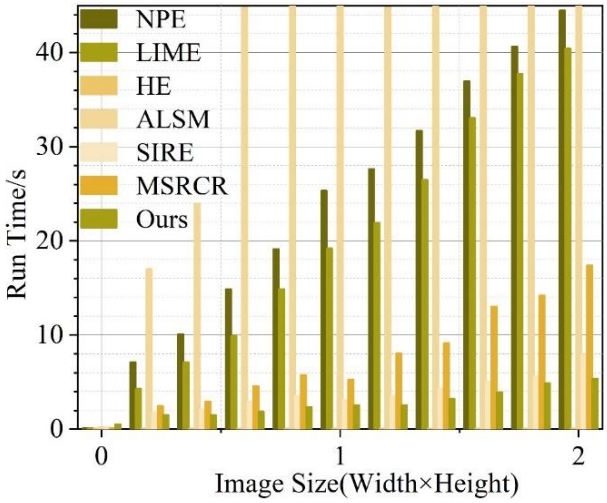

Figure 3: Comparison of the average execution time of different algorithms

4 VGG + Retinex-Net + Improved YOLOv5 for Power Equipment Fault Identification

4.1 YOLOv5 Network Structure

YOLOv5 is a commonly used object detection network, primarily composed of three components: the backbone network, the neck network, and the detection head. The structural diagram of YOLOv5 is shown in Figure 4. The backbone network is responsible for extracting features from the input image to obtain features at different levels. The neck network is located after the backbone network, and its primary function is to enhance the features extracted by the backbone network [35]. The detection head is used to output prediction boxes to assist in object recognition. The YOLOv5 network demonstrates excellent classification and recognition performance, so this paper selects this network as the fault recognition network for power equipment.

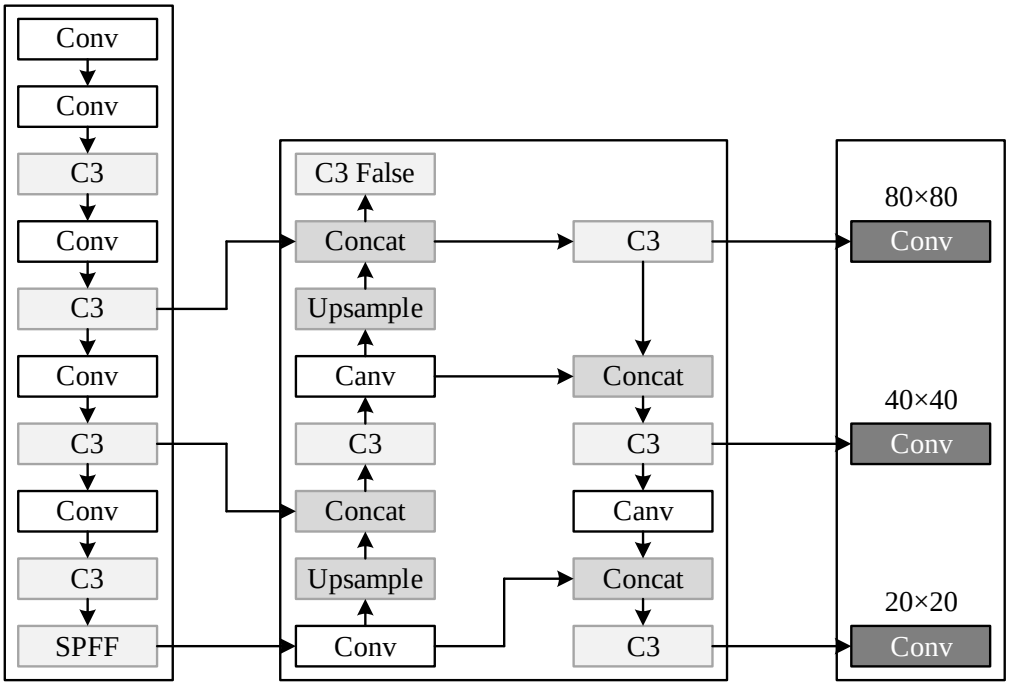

Figure 4: Schematic diagram of the structure of YOLOV5

4.2 Improvements to the VGG Network

During the training process of the VGG network, if there is a significant difference in the amount of data between the training dataset and the testing dataset, it will be difficult for the network to achieve optimal performance. To solve this problem and improve the accuracy of ultra-high voltage substation inspection image classification, the VGG network was first modified. Specifically, a normalization layer was added after each convolutional layer of the VGG network. The normalization layer processes the features extracted by the convolutional layer as follows:

$$\hat{x}_i = \frac{x_i - \mu}{\sqrt{\sigma^2 + \varepsilon}} \tag{8}$$

In the equation: μ is the mean. σ is the variance. $x_i, \hat{x}_i$ are the feature data before and after normalization. ε is a constant.

When ultra-high voltage power equipment images are input into the VGG network, features are extracted through the convolution layer, processed using the added normalization layer, enhanced through the max pooling layer, and finally classified using the fully connected layer, resulting in ultra-high voltage power equipment images under low and normal illumination conditions. The Retinex-Net network is used to enhance low-illumination images, which are then combined with normal-illumination images and input into the YOLOv5 network to achieve fault identification. Since the performance of the YOLOv5 network is related to the loss function, convolution operations, etc., the YOLOv5 network was improved to further enhance fault identification accuracy.

4.3 YOLOv5 Network Improvements

1) Loss function improvement

The loss function has a direct impact on the performance of the YOLOv5 network. The

standard YOLOv5 network loss function typically uses the GIoU function, which has the problem of slow convergence. To solve this problem, the DIoU loss function, which reduces the normalized distance of the center point, is used as a substitute. The formula for the DIoU loss function is:

$$L = 1 - IoU + \frac{\rho^2(b, b^{gt})}{c^2} \tag{9}$$

In the formula: b is the bounding box. b^{gt} is the true box. $\rho^2(b, b^{gt})$ is the Euclidean distance between b and b^{gt}. c is the minimum outer bounding diagonal length of the two boxes.

2) Convolution Improvement

The YOLOv5 network uses conventional convolutions to extract features, which results in a large number of parameters and high computational complexity. Therefore, depth-separable convolutions are introduced to replace conventional convolutions. The process of feature extraction using depth-separable convolutions is as follows: the input image first undergoes three-channel per-channel convolutions to generate three feature values, which are then weighted and combined via per-point convolutions to produce new features. This ensures cross-channel information exchange and spatial information acquisition while minimizing computational and parameter requirements. The structure of depth-separable convolutions is shown in Figure 5.

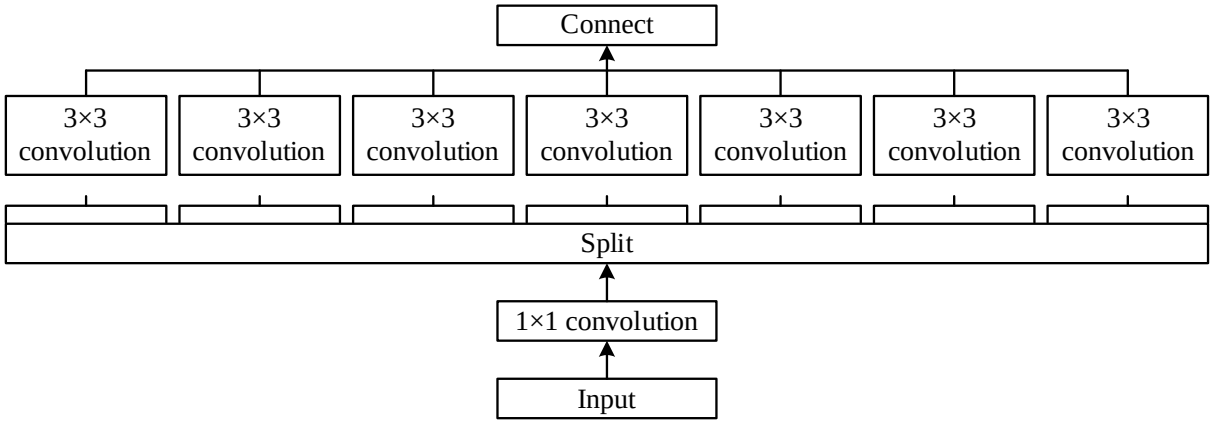

Figure 5: Schematic diagram of the depth-separable convolutional structure

3) Introduction of the attention mechanism

When the standard YOLOv5 network extracts features, it pays equal attention to background features and target features, resulting in some error in the final recognition results. To solve this problem, the CBAM attention mechanism is introduced into the neck network of the YOLOv5 network.

The CBAM attention mechanism is an attention mechanism that calculates feature weights in both the channel and spatial dimensions, enabling enhanced focus on key information in target features. By performing weighted combination on the enhanced features, the objective of strengthening target features is achieved.

4.4 Image Fault Recognition Algorithm Design

Combining the improved VGG network, Retinex-Net network, and improved YOLOv5

network, fault identification is performed on power equipment images. The specific fault identification process is as follows: Image collection. Infrared images of ultra-high-voltage substations captured during intelligent patrol inspections are collected, and the fault categories of the images are annotated. Image classification. The improved VGG network is used to classify the images and filter out low-light images. Image enhancement. The Retinex-Net network is used to enhance low-light images, resulting in enhanced image pairs. Dataset division. All images are mixed and divided into training and testing datasets. Fault identification. The improved YOLOv5 network is trained using the training dataset, and the testing dataset is input into the trained improved YOLOv5 network, with the output results representing the fault identification results [36]. The fault identification algorithm for power equipment is shown in Figure 6.

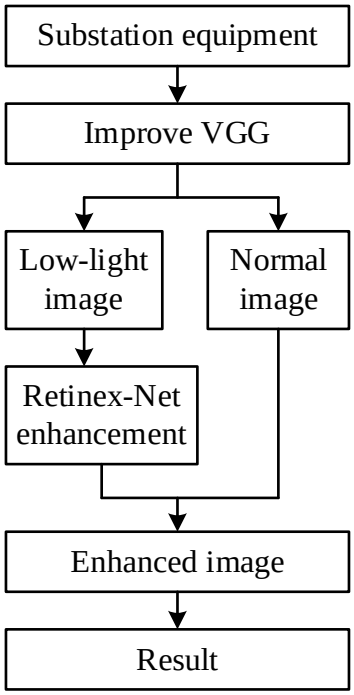

Figure 6: Fault identification algorithm

5 Algorithm performance testing experiment

5.1 Experimental Environment and Evaluation Criteria

The hardware environment used in this experiment is as follows: GPU is NVIDIA 1500Ti with 16GB of video memory, CPU is Intel(R) Core(TM) i7-5009K with 32GB of memory. The software platform selected was the Ten-sorflow deep learning framework, with Python used for program development. Evaluation metrics included accuracy (P), recall (R), and time (S) as indicators for assessing model performance. To validate the algorithm's effectiveness in identifying power equipment faults, this study conducted experiments using six common types of power equipment as fixed samples: high-voltage bushings, current transformers, disconnect switch blades, surge arresters, capacitors, and insulators.

5.2 Ablation experiment

To analyze the impact of different improvement modules on the network model in this paper, six groups of different power equipment images were used as experimental objects, and five

independent ablation experiments were conducted sequentially.

To objectively analyze the ablation experiment results, this paper evaluated them using two objective metrics: spatial frequency (SF) and average gradient (AG). SF is used to evaluate image details, edges, and textures, while AG is used to evaluate image gradients. The ablation experiment results are shown in Table 3. From the table, it can be concluded that improving the loss function, introducing the attention mechanism, and introducing depth-separable convolutions can all enhance the performance metrics of the YOLOv5 network to varying degrees. Additionally, simultaneously improving the loss function and introducing the attention mechanism and depth-separable convolutions yields better performance improvements for the YOLOv5 network. The SF value increased by 361.40%, and the AG value increased by 93.08%. The use of various improvement modules effectively enhances the YOLOv5 network.

Table 3: The results of ablation experimental

Improvement of loss function	Introduction of attention mechanism	The introduction depth can separate convolution	Evaluation index	
			SF	AG
×	×	×	1.0521	2.9192
√	×	×	1.5136	3.0518
×	√	×	4.6859	5.3638
×	×	√	2.1736	3.9146
√	√	√	4.8544	5.6364

5.3 Comparative experiments

Compared with traditional deep learning-based image recognition algorithms such as FusionGAN, CNN, and DenseFuse, the algorithm proposed in this paper provides richer detail information at the connection points between fault locations and power equipment, clearer and more complete fault contours, superior visual effects, and more accurate recognition results. To better evaluate the experimental results, this paper uses four objective metrics: spatial frequency (SF), mutual information (MI), average gradient (AG), and visual information fidelity (VIF). The comparison results are shown in Table 4. MI is used to measure the amount of information retained in the fused image from the original image, while VIF measures image distortion. Compared to the FusionGAN algorithm, the proposed algorithm achieves an average improvement of 0.7867 (19.73%) in SF and 0.4358 (13.01%) in MI. Under the parallel fusion strategy of SA and CA, the fused image exhibits better visual quality and less distortion, with average improvements of 1.0529 (22.60%) and 0.1302 (10.35%) in AG and VIF, respectively. This indicates that the proposed algorithm performs more thorough feature extraction on the fused images, resulting in more complete texture and richer detail information in the fused images.

Table 4: The results of experimental contrasting

Device name	Algorithm model	SF	MI	AG	VIF
Current transformer	FusionGAN	4.5667	4.2463	6.4308	1.1576
	CNN	4.6213	4.6489	5.5645	1.1328
	DenseFuse	4.6045	4.4963	6.1379	1.2142
	Ours	4.6687	4.8907	6.6472	1.2607
High-voltage bushing	FusionGAN	2.739	3.3489	3.6618	1.5107
	CNN	2.8348	3.3769	3.9193	1.5592
	DenseFuse	2.6314	3.3743	3.529	1.471
	Ours	3.5726	3.8975	4.3005	1.5733
Disconnector knife edge	FusionGAN	4.4708	3.5128	4.2565	1.0781
	CNN	4.5564	3.5138	4.2286	1.0527
	DenseFuse	4.3256	3.4745	4.2535	0.9641
	Ours	4.7865	3.855	4.9645	1.1399
Lightning arrester	FusionGAN	4.5799	2.8853	4.9941	1.1212
	CNN	4.5018	3.0911	5.21	0.9628
	DenseFuse	4.7171	2.5173	5.8004	1.0302
	Ours	4.7694	3.0102	6.0709	1.1905
Capacitor	FusionGAN	3.5838	2.7574	3.9531	1.4208
	CNN	3.2424	3.1904	3.7496	1.4181
	DenseFuse	3.246	3.002	4.036	1.4228
	Ours	3.677	3.2363	4.2829	1.5094
Insulator	FusionGAN	7.0386	3.8997	7.7079	1.6876
	CNN	6.7215	3.1209	6.7914	1.416
	DenseFuse	6.769	3.687	7.3741	1.4995
	Ours	7.1742	3.8259	8.0072	1.6532

5.4 Recognition Performance Testing and Results Analysis

To validate the feasibility of the proposed power equipment fault identification method, field-collected data was used for case analysis. First, the commonly encountered fault types were categorized into four categories:

① Battery fault. ② Database fault. ③ Ammeter fault. ④ Power dispatch switch fault. The collected photos were analyzed using the following six model methods for case validation:

Method 1: AR-PCNN-GRU.

Method 2: AR-PCNN-LSTM.

Method 3: AR-PCNN-CNN-GRU.

Method 4: AR-PCNN-CNN-LSTM.

Method 5: AR-OP-CNN-LSTM.

Method 6: The method proposed in this paper.

Through case studies, the diagnostic results of different methods for different fault categories were obtained. The accuracy and recall rates of different methods for fault identification are shown in Tables 5 and 6, respectively. As shown in Tables 5–6, the proposed method in this study achieved the highest accuracy and recall rates in different fault detection scenarios, with average accuracy and recall rates of 0.973 and 0.981, respectively, for the four types of faults. Based on these two metrics, the proposed method can intelligently perceive and detect power equipment faults.

Table 5: The accuracy rates of fault identification by different methods

Method	Fault 1	Fault 2	Fault 3	Fault 4
1	0.936	0.872	0.931	0.926
2	0.951	0.897	0.931	0.919
3	0.924	0.94	0.889	0.962
4	0.914	0.89	0.905	0.945
5	0.979	0.983	0.902	0.97
6	0.995	0.988	0.928	0.982

Table 6: The recall rate of fault identification by different methods

Method	Fault 1	Fault 2	Fault 3	Fault 4
1	0.924	0.945	0.932	0.932
2	0.915	0.956	0.89	0.898
3	0.961	0.941	0.958	0.907
4	0.903	0.955	0.912	0.935
5	0.977	0.976	0.966	0.905
6	0.982	0.981	0.996	0.963

After verifying the feasibility and identification accuracy of the proposed method, a case study analysis was conducted to evaluate its operational efficiency. Each method was run 10 times, and the average detection time for each method under different fault conditions was obtained. The fault identification times for different methods are shown in Table 7. As can be seen from the table, the proposed method has the shortest fault identification time and the highest operational efficiency. Additionally, the proposed algorithm can simultaneously balance detection accuracy and identification efficiency. It demonstrates superior overall performance, enabling rapid and highly accurate detection and identification of power equipment faults.

Table 7: Fault detection time of different methods(s)

Method	Fault 1	Fault 2	Fault 3	Fault 4
1	1.36	1.36	1.61	1.31
2	1.46	1.61	1.59	1.45
3	1.4	1.4	1.43	1.4
4	1.52	1.33	1.46	1.39
5	1.31	1.31	1.4	1.29
6	1.26	1.21	1.12	1.20

6 Conclusion

Under low-light environmental conditions, a fault detection method for power equipment based on image enhancement technology can rapidly and accurately identify faults in circuit breakers, transformers, disconnectors, and bushing connectors. Therefore, this paper proposes an image-based fault detection method utilizing Retinex-Net and an improved YOLOv5 network. The conclusions drawn are as follows:

In ablation experiments, it was found that improving the loss function, introducing an attention mechanism, and incorporating depth-separable convolutions all enhance the performance metrics of the YOLOv5 network to varying degrees. The SF value increased by 361.4%, and the AG value increased by 93.08%. This indicates that the improved modules have

a positive effect on the YOLOv5 network.

Based on the diagnostic results from the case study experiments, the proposed method achieves the highest accuracy and recall rates in various fault detection scenarios, with average values of 0.973 and 0.981, respectively. This demonstrates that the proposed method can intelligently perceive and detect faults in power equipment.

About the Authors

Yihui Zheng, male, 2005-2009, Zhejiang University, majoring in Electrical Engineering and Automation, Bachelor's degree. He focused on neural networks and power grid load forecasting. 2013-2016, South China University of Technology, majoring in electrical engineering, Master's degree. His primary research focused on the application of online monitoring systems in the substation field. As a senior engineer, he is the senior manager of substation operations. With 16 years of specialization in technical management of substation operations, he is engaging in research on the intelligent operations and maintenance technologies for substations. As the first author, he has published 3 core power engineering journals, and participated in development and construction of China Southern Power Grid's pioneering Substation Operational Support System. He has been honored with several awards from Guangzhou Power Supply Bureau, including the First Prize in Management Innovation (2023), the First Prize in the Substation Operation Competition (2012), and specific recognition for Employee Innovation & Achievement Promotion. He has awarded the Third Prize in Employee Innovation from China Southern Power Grid as well.

Chao Sun, male, 2010 - 2013, Zhejiang University, majoring in Power Electronics and Power Drives, Master's Degree. 2014 - 2018, Dalian University of Technology, majoring in Electrical Engineering and Automation, Bachelor's degree. Since 2013, working at Guangzhou Power Supply Bureau, China Southern Power Grid, he has participated in the development of multiple substation intelligent operation and maintenance systems and the reconstruction and construction projects of station-side facilities. These efforts have effectively improved the quality and efficiency of substation equipment operation and maintenance. Responsible for organizing and implementing projects such as the construction and application of intelligent inspection robot systems, the intelligent transformation of remote patrol and operation in substations, and the construction of integrated networking inspection systems for intelligent operation and maintenance of substations. He has been awarded the First Prize for Excellent Papers at the National Power Grid Intelligent Operation and Maintenance Conference and the Second Prize for Innovation Achievements in Equipment Management of the National Electric Power Industry.

Donghai Kuang, male, 1990-1994, South China University of Technology, Bachelor's degree, also earned a Master of engineering degree in SCUT. He is a senior engineer at China Southern Power Grid Co., Ltd. With 32-years of experience in the power industry, he leverages extensive frontline expertise and technical-theoretical proficiency to serve as a key decision-maker in substation operation management. Also focusing on innovative talent management in training evaluation, he established a scientific talent development and competency evaluation system. His promotion of deep training-operation synergy enhances power workforce development. As a deputy director, he spearheaded the team in researching and building China Southern Power Grid's pioneering Substation Operational Support System for substations with demonstrating forward-looking vision and practical expertise, leading advancements in smart substation operation.

Yongbiao Liu, male, 2010-2012, Zhengzhou University, majoring in Electrical Engineering and Automation, Bachelor's Degree, his research focused on digital substation and applications.

With 28-years professional experience in power substation field, he specializes in intelligent operation and maintenance, monitoring technologies, and substation operation management. As a principal creator, he directed the technical retrofit project "Remote Inspection & Operation Intelligent Upgrade of 110kV Jianfeng Substation", and awarded National Class II Innovation Achievement in Power Industry Equipment Management. He has participated in the research and construction of intelligent spatial management and intelligent operation and maintenance in the substation field of the Southern Power Grid.

Peng Xu, male, from Changde, Hunan Province, holds a Master's degree in Electrical Engineering from Huazhong University of Science and Technology. He is a Senior Engineer at China Southern Power Grid Co., Ltd. He has long been dedicated to research on power system equipment, with main research directions focusing on condition monitoring, fault diagnosis, and intelligent upgrade of power equipment, primarily involving research on key power equipment such as transformers and switchgear.

Hai Sun, male, 2012 - 2015, North China Electric Power University, majoring in Power Electronics and Electric Drives, Master's Degree. His research direction was smart microgrid technology. 2008 - 2012, North China Electric Power University, majoring in Electrical Engineering & Automation, Bachelor's degree. Since 2015, working at Guangzhou Power Supply Bureau, engaged in Production & Operations Monitorin and Substation Equipment Maintenance & Testing Work.

References

[1] Lisin, E., Shuvalova, D., Volkova, I., & Strielkowski, W. (2018). Sustainable development of regional power systems and the consumption of electric energy. Sustainability, 10(4), 1111.

[2] Alvarez-Alvarado, M. S., Donaldson, D. L., Recalde, A. A., Noriega, H. H., Khan, Z. A., Velasquez, W., & Rodriguez-Gallegos, C. D. (2022). Power system reliability and maintenance evolution: A critical review and future perspectives. Ieee Access, 10, 51922-51950.

[3] Bie, Z., Lin, Y., Li, G., & Li, F. (2017). Battling the extreme: A study on the power system resilience. Proceedings of the IEEE, 105(7), 1253-1266.

[4] Hrinchenko, H., Koval, V., Shmygol, N., Sydorov, O., Tsimoshynska, O., & Matuszewska, D. (2023). Approaches to sustainable energy management in ensuring safety of power equipment operation. Energies, 16(18), 6488.

[5] Tan, Y., Zhou, L., Xue, X., & Duan, B. (2023). Exploration of Key Technologies for Equipment Operation and Maintenance Based on New Power Systems. International Journal of Thermofluids, 20, 100482.

[6] Kallambettu, J., & Viswanathan, V. (2018). Application of functional safety to electrical power equipment and systems in process industries. Journal of Loss Prevention in the Process Industries, 56, 155-161.

[7] Popa, C. (2020). Impact of substations equipment to the environment. International Journal of Global Warming, 21(2), 155-172.

[8] Chojnacki, A. L. (2023). Analysis of seasonality and causes of equipment and facility

failures in electric power distribution networks. Przeglad Elektrotechniczny, 99(1), 157-163.

[9] Choudhary, M., Shafiq, M., Kiitam, I., Hussain, A., Palu, I., & Taklaja, P. (2022). A review of aging models for electrical insulation in power cables. Energies, 15(9), 3408.

[10] Podobedov, P. N., Nekrasov, A. A., & Maslennikov, P. A. (2019, September). Influence of failure causes of distribution substation power circuit on power supply reliability. In 2019 International Russian Automation Conference (RusAutoCon) (pp. 1-6). IEEE.

[11] Chua, Q. S., & Goh, K. C. (2017). Transmission line fault detection: A review. Indonesian Journal of Electrical Engineering and Computer Science, 8(1), 199-205.

[12] Babak, V. P., Babak, S. V., Eremenko, V. S., Kuts, Y. V., Myslovych, M. V., Scherbak, L. M., & Zaporozhets, A. O. (2021). Models and measures for the diagnosis of electric power equipment. In Models and Measures in Measurements and Monitoring (pp. 99-126). Cham: Springer International Publishing.

[13] Zhao, X., Peng, Z., & Zhao, S. (2020). Substation electric power equipment detection based on patrol robots. Artificial Life and Robotics, 25(3), 482-487.

[14] Sun, Z., Liu, X., Xu, B., Zhang, S., Fu, C., Yang, G., ... & Zhang, C. (2020). Equipment failure detection method of substation based on tunnel robot. Procedia Computer Science, 166, 305-309.

[15] Yao, N., & Wu, X. (2017). Transformer fault detection based on infrared power image. Acta Technica CSAV (Ceskoslovensk Akademie Ved), 62(2), 237-243.

[16] Meradi, S., Benmansour, K., & Laribi, S. (2023). Failure analysis of medium voltage underground power Câbles based on voltage measurements. Journal of Failure Analysis and Prevention, 23(5), 1860-1868.

[17] Wu, H., Shang, W., He, C., Li, B., & Song, K. (2024, February). Design of Power Equipment Fault Detection and Diagnosis System Based on Deep Learning. In 2024 International Conference on Electrical Drives, Power Electronics & Engineering (EDPEE) (pp. 911-916). IEEE.

[18] Liu, T., Li, G., & Gao, Y. (2022). Fault diagnosis method of substation equipment based on You Only Look Once algorithm and infrared imaging. Energy Reports, 8, 171-180.

[19] Li, Y., Wang, T., Yang, G., Yuan, H., & Wang, D. (2021). RESEARCH ON FAULT IDENTIFICATION OF POWER EQUIPMENT BASED ON BP NEURAL NETWORK. International Journal of Mechatronics and Applied Mechanics, (9), 51-57.

[20] Liu, Y., Li, F., Guan, Q., Zhao, Y., & Yan, S. (2022). Power equipment fault diagnosis method based on energy spectrogram and deep learning. Sensors, 22(19), 7330.

[21] Liu, J., Xu, C., Ye, Q., Cao, L., Dai, X., & Li, Q. (2024). Thermal imaging-based abnormal heating detection for high-voltage power equipment. Energies, 17(16), 4035.

[22] Zhou, F., Ma, Y., Ma, Y., & Pan, H. (2020, March). Infrared image fault identification of

power equipment based on residual network. In Workshops of the International Conference on Advanced Information Networking and Applications (pp. 3-13). Cham: Springer International Publishing.

[23] Guan, X., Gao, W., Peng, H., Shu, N., & Gao, D. W. (2021). Image-based incipient fault classification of electrical substation equipment by transfer learning of deep convolutional neural network. IEEE Canadian Journal of Electrical and Computer Engineering, 45(1), 1-8.

[24] Zhong, J., Chen, Y., Gao, J., & Lv, X. (2024). Drone image recognition and intelligent power distribution network equipment fault detection based on the transformer model and transfer learning. Frontiers in Energy Research, 12, 1364445.

[25] Zhao, Y., Wu, J., Chen, W., Wang, Z., Tian, Z., Yu, F. R., & Leung, V. C. (2024). A small object real-time detection method for power line inspection in low-illuminance environments. IEEE Transactions on Emerging Topics in Computational Intelligence, 8(6), 3936-3950.

[26] Rundo, L., Tangherloni, A., Nobile, M. S., Militello, C., Besozzi, D., Mauri, G., & Cazzaniga, P. (2019). MedGA: a novel evolutionary method for image enhancement in medical imaging systems. Expert Systems with Applications, 119, 387-399.

[27] Wang, Q., Hu, Q., Qiu, J., Pei, C., Li, X., Zhou, H., ... & Liu, J. (2019). Image enhancement method for laser infrared thermography defect detection in aviation composites. Optical Engineering, 58(10), 103104-103104.

[28] Ablin, R., Sulochana, C. H., & Prabin, G. (2020). An investigation in satellite images based on image enhancement techniques. European Journal of Remote Sensing, 53(sup2), 86-94.

[29] Khemani, L. P., Yadav, R. K., & Doshi, T. V. (2025). Novel Optimized Image Enhancement and Deep Learning Based Crack Detection Algorithm in Non-Destructive Testing. Indian Journal of Science and Technology, 18(7), 487-503.

[30] Prasad, K. K., & Aithal, P. S. (2017). A conceptual study on image enhancement techniques for fingerprint images. International Journal of Applied Engineering and Management Letters (IJAEML), 1(1), 63-72.

[31] Liu, D. N., Hou, R., Wu, W. Z., Hua, J. W., Wang, X. Y., & Pang, B. (2019). Research on infrared image enhancement and segmentation of power equipment based on partial differential equation. Journal of Visual Communication and Image Representation, 64, 102610.

[32] Yuan, Z., Zeng, J., Wei, Z., Jin, L., Zhao, S., Liu, X., ... & Zhou, G. (2023). CLAHE-based low-light image enhancement for robust object detection in overhead power transmission system. IEEE Transactions on Power Delivery, 38(3), 2240-2243.

[33] Yao Lu. (2025). LSEVGG: An attention mechanism and lightweight-improved VGG network for remote sensing landscape image classification. Alexandria Engineering Journal,127,943-951.

[34] Feng Wei,Wu Guiming,Zhou Shiqi & Li Xingang. (2023). Low-light image enhancement based on Retinex-Net with color restoration.. Applied optics,62(25),6577-6584.

[35] Danqing Ma,Shaojie Li,Bo Dang,Hengyi Zang & Xinqi Dong. (2024). Fostc3net: A lightweight YOLOv5 based on the network structure optimization. Journal of Physics: Conference Series,2824(1),012004-012004.

[36] Jie Song,Xinyan Qin,Jin Lei,Jie Zhang,Yanqi Wang & Yujie Zeng. (2024). A fault detection method for transmission line components based on synthetic dataset and improved YOLOv5.International Journal of Electrical Power and Energy Systems, 157, 109852-.